Polymerization of Lactide with Zinc and Magnesium β-Diiminate Complexes: Stereocontrol and Mechanism

Bradley M. Chamberlain, Ming Cheng, David R. Moore, Tina M. Ovitt, Emil B. Lobkovsky, and Geoffrey W. Coates*

Contribution from the Department of Chemistry and Chemical Biology, Baker Laboratory, Cornell University, Ithaca, New York 14853-1301

Received November 1, 2000

Abstract: A series of zinc(II) and magnesium(II) alkoxides based upon a β-diiminate ligand framework has been prepared. [(BDI-**1**)ZnO^{i}Pr]$_2$ [(BDI-**1**) = 2-((2,6-diisopropylphenyl)amido)-4-((2,6-diisopropylphenyl)-imino)-2-pentene] exhibited the highest activity and stereoselectivity of the zinc complexes studied for the polymerization of *rac*- and *meso*-lactide to poly(lactic acid) (PLA). [(BDI-**1**)ZnO^{i}Pr]$_2$ polymerized (*S*,*S*)-lactide to isotactic PLA without epimerization of the monomer, *rac*-lactide to heterotactic PLA (P_r = 0.94 at 0 °C), and *meso*-lactide to syndiotactic PLA (P_r = 0.76 at 0 °C). The polymerizations are living, as evidenced by the narrow polydispersities of the isolated polymers in addition to the linear nature of number average molecular weight versus conversion plots and monomer-to-catalyst ratios. The substituents on the β-diiminate ligand exert a significant influence upon the course of the polymerizations, affecting both the degree of stereoselectivity and the rate of polymerization. Kinetic studies with [(BDI-**1**)ZnO^{i}Pr]$_2$ indicate that the polymerizations are first order with respect to monomer (*rac*-lactide) and 1.56 order in catalyst. Polymerization experiments with [(BDI-**1**)MgO^{i}Pr]$_2$ revealed that this complex is extremely fast for the polymerization of *rac*-lactide, polymerizing 500 equiv in 96% yield in less than 5 min at 20 °C.

Introduction

Although remarkable advances have been reported concerning the development of single-site metal catalysts for olefin polymerization,[1] relatively few well-defined metal catalysts are available for the ring-opening polymerization of heterocycles such as lactide.[2−14] Because the stereochemistry of poly(lactic acids) (PLA) determines both their mechanical and physical properties, as well as their rates of chemical and biological degradation, the synthesis of new microstructures may lead to new applications for PLA.[15] Prior to work in our laboratory, a range of metal alkoxide initiators was reported to polymerize lactide (LA) with retention of configuration by cleaving the acyl−oxygen bond via a coordination-insertion mechanism.[16−20] Nonetheless, these catalysts were limited to producing only atactic, partially heterotactic, or isotactic microstructures (Figure 1). For example, polymerization of *rac*- or *meso*-lactide with aluminum tris(alkoxides)[19] or tin bis(carboxylates)[20] yields amorphous, atactic polymers with random placements of either −(*RR*)− and −(*SS*)− stereosequences for *rac*-lactide or −(*RS*)− and −(*SR*)− stereosequences for *meso*-lactide. Kasperczyk has reported that LiO^{t}Bu produces predominantly heterotactic PLA from *rac*-lactide.[21,22] In contrast, in the absence of epimerization reactions, polymerization of optically active (*S*,*S*)-lactide (or (*R*,*R*)-lactide) affords crystalline, isotactic polymers. More recently, we have reported routes to syndiotactic[4] and stereoblock isotactic[23] PLAs using chiral aluminum catalysts.

(1) Coates, G. W. *Chem. Rev.* **2000**, *100*, 1223−1252.

(2) Single-site catalysts are those polymerization catalysts where enchainment of monomer occurs at a metal center (M, the active site) which is bound by an organic ligand (L). This ancillary ligand remains bound throughout the catalytic reaction, modifying the reactivity of the metal center. Typical single-site catalysts for lactone polymerization are of the form L_nMOR, where the alkoxide group (OR) is capable of propagation. These complexes are of a different class than typical lactone polymerization catalysts of the form $M(OR)_n$, where all of the ligands are capable of forming a polymer chain and no permanent ligand is present. For recent examples of single-site catalysts for lactone polymerization, see refs 3−14.

(3) Cheng, M.; Attygalle, A. B.; Lobkovsky, E. B.; Coates, G. W. *J. Am. Chem. Soc.* **1999**, *121*, 11583−11584.

(4) Ovitt, T. M.; Coates, G. W. *J. Am. Chem. Soc.* **1999**, *121*, 4072−4073.

(5) Chamberlain, B. M.; Sun, Y. P.; Hagadorn, J. R.; Hemmesch, E. W.; Young, V. G.; Pink, R.; Hillmyer, M. A.; Tolman, W. B. *Macromolecules* **1999**, *32*, 2400−2402.

(6) Spassky, N.; Wisniewski, M.; Pluta, C.; Le Borgne, A. *Macromol. Chem. Phys.* **1996**, *197*, 2627−2637.

(7) Chisholm, M. H.; Eilerts, N. W. *Chem. Commun.* **1996**, 853−854.

(8) Radano, C. P.; Baker, G. L.; Smith, M. R. *J. Am. Chem. Soc.* **2000**, *122*, 1552−1553.

(9) Chamberlain, B. M.; Jazdzewski, B. A.; Pink, R.; Hillmyer, M. A.; Tolman, W. B. *Macromolecules* **2000**, *33*, 3970−3977.

(10) Aida, T.; Inoue, S. *Acc. Chem. Res.* **1996**, *29*, 39−48.

(11) Beckerle, K.; Hultzsch, K. C.; Okuda, J. *Macromol. Chem. Phys.* **1999**, *200*, 1702−1707.

(12) Yasuda, H.; Ihara, E. *Adv. Polym. Sci.* **1997**, *133*, 53−101.

(13) Ko, B. T.; Lin, C. C. *Macromolecules* **1999**, *32*, 8296−8300.

(14) Chisholm, M. H.; Eilerts, N. W.; Huffman, J. C.; Iyer, S. S.; Pacold, M.; Phomphrai, K. *J. Am. Chem. Soc.* **2000**, *122*, 11845−11854.

(15) PLA materials have already found many medical, agricultural, and packaging applications. For recent examples, see: (a) Chiellini, E.; Solaro, R. *Adv. Mater.* **1996**, *29*, 1375−1381. (b) Ikada, Y.; Tsuji, H. *Macromol. Rapid Commun.* **2000**, *21*, 117−132. (c) Vert, M.; Li, S. N.; Spenlenhauer, G.; Guerin, P. J. *Pure Appl. Chem.* **1995**, *A32*, 787−796.

(16) Kricheldorf, H. R.; Lee, S. R.; Bush, S. *Macromolecules* **1996**, *29*, 1375−1381.

(17) Stevels, W. M.; Dijkstra, P. J.; Feijen, J. *Trends Polym. Sci.* **1997**, *5*, 300−305.

(18) Dubois, P.; Jacobs, C.; Jérôme, R.; Tessié, P. *Macromolecules* **1991**, *24*, 2266−2270.

(19) Kowalski, A.; Duda, A.; Penczek, S. *Macromolecules* **1998**, *31*, 2114−2122.

(20) Kowalski, A.; Duda, A.; Penczek, S. *Macromolecules* **2000**, *33*, 689−695.

(21) Bero, M.; Dobrzynski, P.; Kasperczyk, J. *J. Polym. Sci., Part A* **1999**, *37*, 4038−4042.

(22) Kasperczyk, J. E. *Macromolecules* **1995**, *28*, 3937−3939.

10.1021/ja003851f CCC: $20.00
Published on Web 03/16/2001

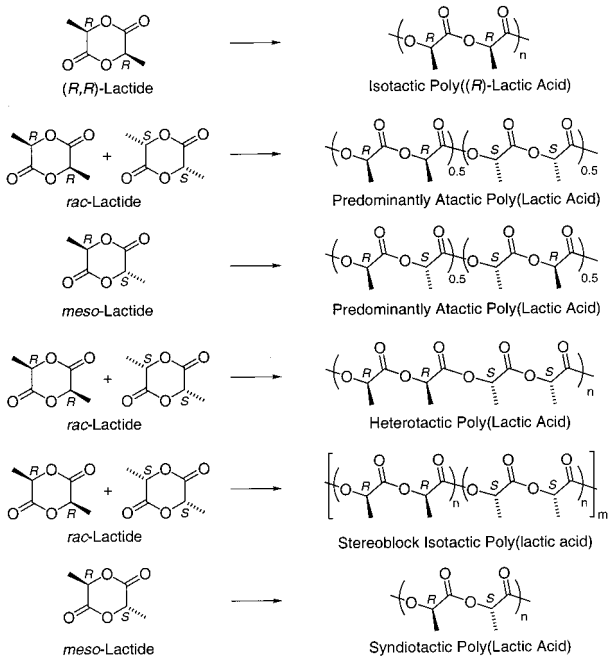

Figure 1. Lactide stereochemistry and PLA microstructures.

On the basis of the observation of earlier classes of polymerization catalysts,[24] we anticipated that zinc complexes[25] ligated by bulky β-diiminate ligands (BDI) might be capable of stereochemical control in the polymerization of *rac*- and *meso*-lactide via a chain-end control mechanism. In such a reaction, the bulky ligands increase the influence of the stereogenic center of the last inserted monomer, which in turn determines the relative sequence of stereocenters in the main chain. Although stereocontrol of this type is conceptually simple, typically only a modest degree of chain-end control during lactide polymerization has been reported.[21,22,26−29] However, we recently communicated the synthesis of a zinc alkoxide complex that acted as a single-site catalyst for the preparation of heterotactic PLA;[3] herein we report the kinetics of polymerization for this catalyst, along with the effect of initiating groups and ligand substituents upon the rate and stereoselectivity of lactide polymerization.[30]

Results and Discussion

Complex Synthesis and Analysis. The isostructural zinc amides (BDI-**1**)ZnN(SiMe$_3$)$_2$, (BDI-**2**)ZnN(SiMe$_3$)$_2$, and (BDI-**3**)ZnN(SiMe$_3$)$_2$ were prepared by treatment of the appropriate ligand with stoichiometric Zn[N(SiMe$_3$)$_2$]$_2$ in toluene at 80 °C (Scheme 1). Complexes (BDI-**1**)ZnN(SiMe$_3$)$_2$ and (BDI-**2**)ZnN(SiMe$_3$)$_2$ were isolated as crystalline solids in 53% and 62% yield, respectively. Complex (BDI-**3**)ZnN(SiMe$_3$)$_2$ was isolated as an oil in quantitative yield; attempts to crystallize (BDI-**3**)ZnN(SiMe$_3$)$_2$ from all common solvents were unsuccessful. X-ray diffraction analysis was performed on crystals of (BDI-**1**)ZnN(SiMe$_3$)$_2$, and the structure was found to be a rare three-coordinate species.[31] ^{1}H NMR spectroscopic data (C$_6$D$_6$, 300 MHz) for (BDI-**1**)ZnN(SiMe$_3$)$_2$, (BDI-**2**)ZnN(SiMe$_3$)$_2$, and (BDI-**3**)ZnN(SiMe$_3$)$_2$ show one symmetrical species each in solution; on the basis of the similarity of their ^{1}H NMR spectra to (BDI-**1**)ZnN(SiMe$_3$)$_2$, (BDI-**2**)ZnN(SiMe$_3$)$_2$ and (BDI-**3**)ZnN(SiMe$_3$)$_2$ are thus also assigned a three-coordinate structure.

Treatment of the zinc amides with stoichiometric 2-propanol in toluene resulted in the release of HN(SiMe$_3$)$_2$ along with concomitant formation of the three isostructural zinc alkoxides [(BDI-**1**)ZnO^{i}Pr]$_2$, [(BDI-**2**)ZnO^{i}Pr]$_2$, and [(BDI-**3**)ZnO^{i}Pr]$_2$ in 54%, 67%, and 54% isolated yield, respectively (Scheme 1). X-ray diffraction analysis had previously revealed the molecular structure of [(BDI-**1**)ZnO^{i}Pr]$_2$ to be a dimeric species wherein isopropoxide ligands bridge distorted tetrahedral zinc centers.[3] X-ray diffraction analyses of crystals of [(BDI-**2**)ZnO^{i}Pr]$_2$ and [(BDI-**3**)ZnO^{i}Pr]$_2$ grown from toluene revealed analogous dimeric structures, with no significant perturbations of the Zn$_2$O$_2$ core across the ligand series. For example, the Zn···Zn separation in [(BDI-**1**)ZnO^{i}Pr]$_2$ [3.099 Å] is slightly larger than that in [(BDI-**3**)ZnO^{i}Pr]$_2$ [2.990 Å].[32] ^{1}H NMR spectroscopic data (C$_6$D$_6$, 300 MHz) for [(BDI-**1**)ZnO^{i}Pr]$_2$, [(BDI-**2**)ZnO^{i}Pr]$_2$, and [(BDI-**3**)ZnO^{i}Pr]$_2$ show one symmetrical species each in solution; on the basis of solution exchange experiments between related methoxide complexes,[33] we propose that all three alkoxides retain their dimeric structures in solution.

Treatment of the zinc amide (BDI-**1**)ZnN(SiMe$_3$)$_2$ with stoichiometric *rac*-methyl lactate in toluene resulted in the isolation of the novel complex *rac*-(BDI-**1**)ZnOCH(Me)CO$_2$Me as colorless blocks in 41% yield (Scheme 1). The molecular structure of *rac*-(BDI-**1**)ZnOCH(Me)CO$_2$Me, as determined by X-ray diffraction, is a monomeric species wherein the zinc center is ligated in a distorted tetrahedral array by one β-diiminate ligand and one methyl lactate moiety (Figure 2).[32] Both the alkoxide and carbonyl oxygen atoms of the methyl lactate ligand coordinate the zinc center, although the distance of the dative Zn−carbonyl bond [Zn(1)−O(2) = 2.189 Å] is significantly longer than that of the Zn−alkoxide bond [Zn(1)−O(1) = 1.879 Å]. ^{1}H NMR spectroscopic data (C$_6$D$_6$, 300 MHz) for *rac*-(BDI-**1**)ZnOCH(Me)CO$_2$Me exhibit four inequivalent CH*Me*$_2$ shifts; we tentatively propose that the monomeric species is retained in solution.

Treatment of (BDI-**1**)H with ZnEt$_2$ in toluene at 70 °C followed by removal of solvent in vacuo resulted in the formation of (BDI-**1**)ZnEt as a viscous yellow-brown oil in

(23) Ovitt, T. M.; Coates, G. W. *J. Polym. Sci., Part A* **2000**, *38*, 4686−4692.

(24) For some recent examples of polymerization catalysts with bulky ligands that control stereochemistry by a chain-end control mechanism, see: (a) Small, B. L.; Brookhart, M. *Macromolecules* **1999**, *32*, 2120−2130. (b) Resconi, L.; Franciscono, G. *Macromolecules* **1992**, *25*, 6814−6817.

(25) For some examples of zinc-based catalysts for lactone polymerization, see: (a) Watanabe, Y.; Yasuda, T.; Aida, T.; Inoue, S. *Macromolecules* **1992**, *25*, 1396−1400. (b) Barakat, I.; Dubois, P.; Jerome, R.; Teyssie, P. *Macromolecules* **1991**, *24*, 6542−6545. (c) Nijenhuis, A. J.; Grijpma, D. W.; Pennings, A. J. *Polym. Bull.* **1991**, *26*, 71−77. (d) Noltes, J. G.; Verbeek, F.; Overmars, H. G.; Boersma, J. *J. Organomet. Chem.* **1970**, *24*, 257−267. (e) Kricheldorf, H. R.; Damrau, D. O. *Macromol. Chem. Phys.* **1998**, *199*, 1747−1752. (f) Schwach, G.; Coudane, J.; Engel, R.; Vert, M. *Polym. Int.* **1998**, *46*, 177−182.

(26) Thakur, K. A. M.; Kean, R. T.; Hall, E. S.; Kolstad, J. J.; Lindgren, T. A.; Doscotch, M. A.; Siepmann, J. I.; Munson, E. J. *Macromolecules* **1997**, *30*, 2422−2428.

(27) Thakur, K. A. M.; Kean, R. T.; Hall, E. S.; Kolstad, J. J.; Munson, E. J. *Macromolecules* **1998**, *31*, 1487−1494.

(28) Wisniewski, M.; Le Borgne, A.; Spassky, N. *Macromol. Chem. Phys.* **1997**, *198*, 1227−1238.

(29) Coudane, J.; Ustariz-Peyret, C.; Schwach, G.; Vert, M. *J. Polym. Sci., Part A* **1997**, *35*, 1651−1658.

(30) (BDI)MOR (M = Mg, Zn) catalysts are also active for the polymerization of other lactones, such as ϵ-caprolactone and β-butyrolactone (manuscript in preparation).

(31) For other examples of three-coordinate zinc complexes, see: (a) Gorrel, I. B.; Looney, A.; Parkin, G.; Rheingold, A. L. *J. Am. Chem. Soc.* **1990**, *112*, 4068−4069. (b) Gruff, E. S.; Koch, S. A. *J. Am. Chem. Soc.* **1989**, *111*, 8762−8763. (c) Al-Juaid, S. S.; Buttrus, N. H.; Eaborn, C.; Hitchcock, P. B.; Roberts, A. T. L.; Smith, J. D. S.; Sullivan, A. C. *J. Am. Chem. Soc.* **1986**, *108*, 908−909.

(32) See Supporting Information.

(33) Coates, G. W. et al. Manuscript in preparation.

Scheme 1

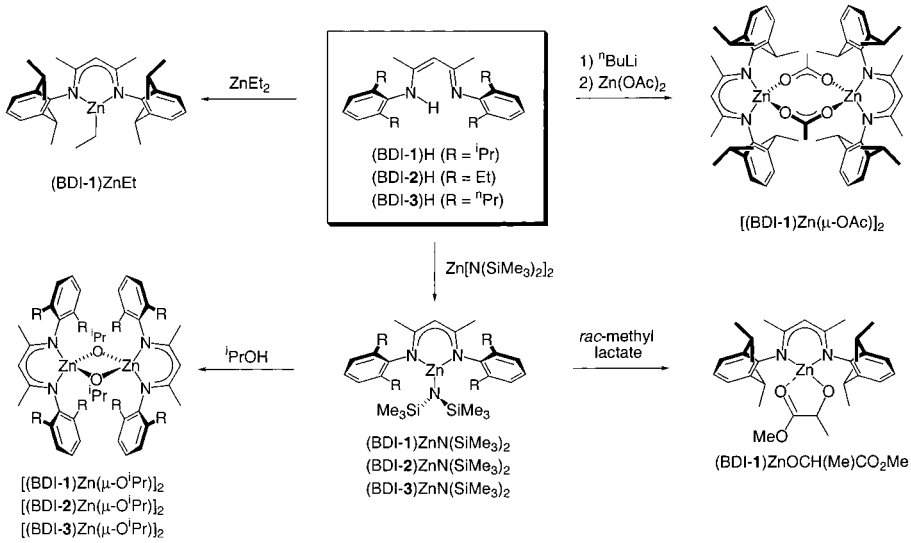

Table 1. Effect of Initiating Group: (BDI-1)ZnX with *rac*-Lactide[a]

entry	catalyst	time (h)	conversion[b] (%)	M_n (kg/mol) (GPC)[c]	M_w/M_n (GPC)[c]
1	(BDI-**1**)ZnN(SiMe$_3$)$_2$	10	97	33.6	2.95
2	[(BDI-**1**)ZnO^{i}Pr]$_2$	0.33	95	37.9	1.10
3	*rac*-(BDI-**1**)ZnOCHMeCO$_2$Me	0.33	97	30.5	1.14
4	(BDI-**1**)ZnEt	20	97	63.3	1.83
5	[(BDI-**1**)ZnOAc]$_2$	70	92	61.4	2.07

[a] [LA]/[Zn] = 200; T_{rxn} = 20 °C; [LA] = 0.4 M in CH_2Cl_2. [b] As determined via integration of the methyl resonances of LA and poly-LA ($CDCl_3$, 300 MHz). [c] Determined by gel-permeation chromatography, calibrated with polystyrene standards in tetrahydrofuran.

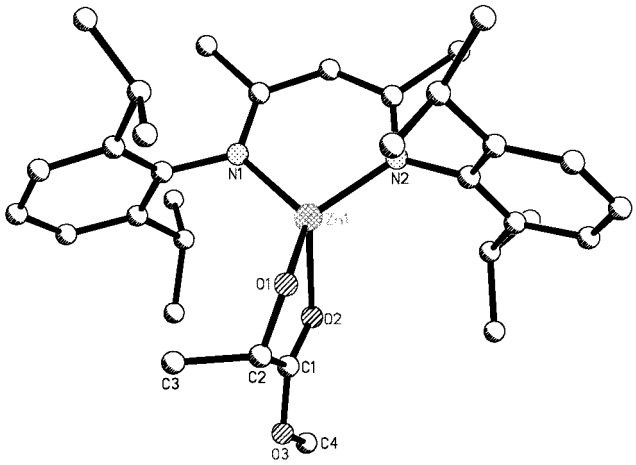

Figure 2. Molecular structure of *rac*-(BDI-**1**)ZnOCH(Me)CO$_2$Me. Selected bond distances (Å) and angles (deg): Zn(1)−N(1) 1.977(3), Zn(1)−N(2) 1.952(2), Zn(1)−O(1) 1.879(2), Zn(1)−O(2) 2.189(2), C(1)−O(2) 1.226(4), C(2)−O(1) 1.391(4), N(1)−Zn(1)−N(2) 99.67(1), O(1)−Zn(1)−O(2) 82.44(9), N(1)−Zn(1)−O(1) 124.67(10), N(2)−Zn(1)−O(2), 112.62(9), Zn(1)−O(1)−C(2), 114.7(2), Zn(1)−O(2)−C(1) 105.3(2).

quantitative yield,[33] while treatment of (BDI-**1**)H with *n*-butyllithium followed by Zn(OAc)$_2$ resulted in the isolation of [(BDI-**1**)ZnOAc]$_2$ (Scheme 1).[34]

Effect of Initiating Group upon Lactide Polymerization. Complexes (BDI-**1**)ZnN(SiMe$_3$)$_2$, [(BDI-**1**)ZnO^{i}Pr]$_2$, *rac*-(BDI-**1**)ZnOCH(Me)CO$_2$Me, (BDI-**1**)ZnEt, and [(BDI-**1**)ZnOAc]$_2$ were examined for polymerization activity with *rac*-lactide ([LA]/[Zn] = 200; Table 1). From the polymerization data, it is apparent that the identity of the initiating group significantly affects both the molecular weight and the polydispersity of the polymers. In particular, −N(SiMe$_3$)$_2$, −Et, and −OAc are clearly inferior initiating units, as they yield polymers with broad polydispersities and molecular weights that compare poorly with theoretical values. Unlike −O^{i}Pr and −OCH(Me)CO$_2$Me, initiation with these three species most likely does not occur by direct insertion of the moiety into the acyl−oxygen bond. Rather, these groups likely slowly react with monomer impurities (e.g., lactic acid, hydrolyzed lactide, water) to form a new initiating group. Consequently, the rate of initiation (k_i) is slower than the propagating rate of polymerization (k_p), resulting in polymers with broad molecular weight distributions and higher than expected molecular weights. In contrast, the isopropoxide and methyl lactate initiating groups closely mimic the putative propagating groups of the presumed active species, and complexes with these moieties produce PLA of predictable molecular weight and narrow molecular weight distribution. As [(BDI-**1**)ZnO^{i}Pr]$_2$ is both the easiest and least expensive to access, all complexes discussed subsequently will possess isopropoxide propagating units.

Stereochemistry of Lactide Polymerization with (BDI)-ZnO^{i}Pr Catalysts. According to Bernoullian statistics, PLA derived from both *rac*- and *meso*-lactide possesses five tetrad sequences in relative ratios determined by the ability of the catalyst to control racemic [*r*-dyad] and meso [*m*-dyad] connectivity of the monomer units (Schemes 2 and 3, Table 2).[35] Determination of the stereochemical microstructures of PLA is achieved through inspection of the methine region of homonuclear decoupled ^{1}H NMR spectra of the polymers.[26,36,37] Thus,

(34) Cheng, M.; Lobkovsky, E. B.; Coates, G. W. *J. Am. Chem. Soc.* **1998**, *120*, 11018−11019.

(35) Bovey, F. A.; Mirau, P. A. *NMR of Polymers*; Academic Press: San Diego, 1996.

(36) Thakur, K. A. M.; Kean, R. T.; Zell, M. T.; Padden, B. E.; Munson, E. J. *Chem. Commun.* **1998**, 1913−1914.

Scheme 2

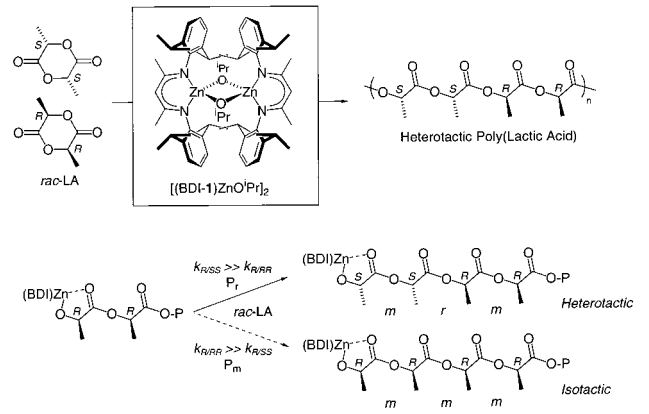

Scheme 3

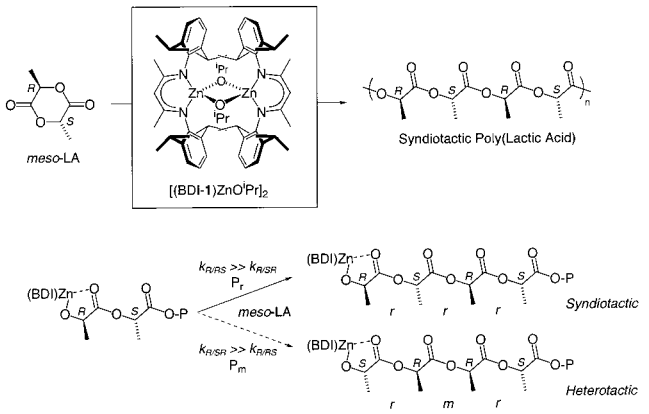

Table 2. Tetrad Probabilities Based on Bernoullian Statistics

	probability	
tetrad	*rac*-lactide	*meso*-lactide
[*mmm*]	$P_m^2 + P_rP_m/2$	0
[*mmr*]	$P_rP_m/2$	0
[*rmm*]	$P_rP_m/2$	0
[*rmr*]	$P_r^2/2$	$(P_m^2 + P_rP_m)/2$
[*rrr*]	0	$P_r^2 + P_rP_m/2$
[*rrm*]	0	$P_rP_m/2$
[*mrr*]	0	$P_rP_m/2$
[*mrm*]	$(P_r^2 + P_rP_m)/2$	$P_m^2/2$

although atactic PLA exhibits five resonances in its ^{1}H NMR spectrum, perfectly heterotactic PLA (Scheme 2) shows only *rmr* and *mrm* tetrads. [(BDI)ZnO^{i}Pr]$_2$ complexes polymerize (*S*,*S*)-lactide to isotactic PLA without observable epimerization. Microstructural analysis of PLA formed from *rac*-lactide with [(BDI-**1**)ZnO^{i}Pr]$_2$ revealed that the complex exerts a significant influence on the tacticity of the growing polymer chain (Figure 3). Two scenarios are possible: if a chain end of *R* stereochemistry selects (*R*,*R*)-lactide (meso enchainment; $k_{R/RR} \gg k_{R/SS}$), then isotactic PLA forms; if this chain end selects (*S*,*S*)-lactide (racemic enchainment; $k_{R/SS} \gg k_{R/RR}$), then heterotactic[38] PLA forms (Scheme 2). PLA produced by [(BDI-**1**)ZnO^{i}Pr]$_2$ at 20 °C is substantially heterotactic with a P_r of 0.90 (entry 1, Table 3).[39] In other words, the probability of a (*R*,*R*)-lactide unit to be enchained after a (*S*,*S*)-lactide unit (or vice versa) is 90%.[40] Upon cooling the reaction mixture to 0 °C, P_r can be improved to 0.94 (entry 4, Table 3). Furthermore, the polymerization data indicate that the substituents on the β-diiminate ligand significantly affect the ability of the catalyst to control monomer enchainment (entries 1−3, Table 3). For instance, changing the ligand substituents from isopropyl to ethyl groups results in a decrease in heterotacticity ($P_r = 0.79$). Similarly, substitution with *n*-propyl groups lowers the heterotacticity ($P_r = 0.76$).

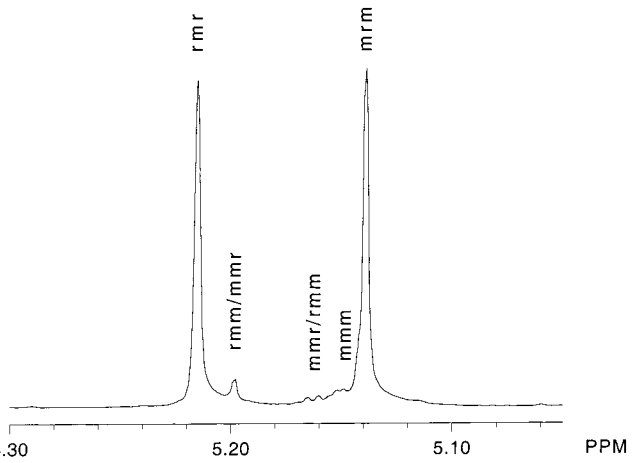

Figure 3. Homonuclear decoupled ^{1}H NMR spectrum of the methine region of heterotactic PLA prepared from *rac*-LA with [(BDI-**1**)ZnO^{i}Pr]$_2$ at 0 °C (500 MHz, $CDCl_3$).

In contrast, polymerization of *meso*-lactide with [(BDI-**1**)ZnO^{i}Pr]$_2$ affords syndiotactic PLA (Scheme 3). According to Bernoullian statistics, syndiotactic polymers may be prepared from *meso*-lactide provided that the propagating chain end shows a propensity for *r*-dyad placement between monomer units (Table 2). Interestingly, [(BDI-**1**)ZnO^{i}Pr]$_2$ produces syndiotactic PLA from *meso*-lactide, while [(BDI-**2**)ZnO^{i}Pr]$_2$ produces moderately *heterotactic* PLA. The origins for the dramatic change in tacticity are not understood at the current time, although we anticipate a possible variance in their detailed mechanisms of enchainment. From the polymerization data (entry 5, Table 3), it is apparent that PLA prepared from *meso*-lactide with [(BDI-**1**)ZnO^{i}Pr]$_2$ (76% racemic linkages between monomer units) is less syndiotactic than that prepared with a chiral Schiff base complex of aluminum (96% racemic linkages between monomer units).[4] Nonetheless, [(BDI-**1**)ZnO^{i}Pr]$_2$ illustrates novel chain-end stereocontrol during the polymerization of *meso*-lactide (Figure 4). Therefore, [(BDI-**1**)ZnO^{i}Pr]$_2$ provides access to syndiotactic PLA microstructures without the use of expensive chiral ligands.

Mechanism and Kinetics of Lactide Polymerization with [(BDI-1)ZnO^{i}Pr]$_2$. Aliquots periodically withdrawn from a polymerization of *rac*-lactide with [(BDI-**1**)ZnO^{i}Pr]$_2$ were used to construct a plot of M_n versus conversion ([Zn] = 0.8 mM; [LA] = 0.4 M; [LA]/[Zn] = 500; Figure 5). The linear nature of this plot, in conjunction with the narrow polydispersities ($M_w/M_n < 1.10$), suggests that the polymerization is living and proceeds by a coordination-insertion mechanism.[41] Furthermore,

(37) Chisholm, M. H.; Iyer, S. S.; Matison, M. E.; McCollum, D. G.; Pagel, M. *Chem. Commun.* **1997**, 1999−2000.

(38) Heterotactic macromolecules are a rare type of polymer that have alternating pairs of stereogenic centers in the main chain (i.e., only *mr*/*rm* triads are observed). See: (a) Hirano, T.; Yamaguchi, H.; Kitayama, T.; Hatada, K. *Polym. J.* **1998**, *30*, 767−769. (b) Yamada, K.; Nakano, T.; Okamoto, Y. *Macromolecules* **1998**, *31*, 7598−7605. (c) Kitayama, T.; Hirano, T.; Hatada, K. *Tetrahedron* **1997**, *53*, 15263−15279. (d) Nakahama, S.; Kobayashi, M.; Ishizone, T.; Hirao, A. *J. Macromol. Sci., Pure Appl. Chem.* **1997**, *A34*, 1845−1855. (e) Fossum, E.; Matyjaszewski, K. *Macromolecules* **1995**, *28*, 1618−1625.

(39) Even when the initiating group perfectly mimics a putative lactide chain end (as in *rac*-(BDI-**1**)ZnOCH(Me)CO$_2$Me), P_r values are identical to those produced by (BDI-**1**)ZnO^{i}Pr at 20 °C.

(40) P_r can also be expressed in terms of the enchainment rate constants: $P_r = k_{R/SS}/(k_{R/SS} + k_{R/RR}) = k_{S/RR}/(k_{S/RR} + k_{S/SS})$.

(41) Stevels, W. M.; Ankoné, M. J. K.; Dijkstra, P. J.; Feijen, J. *Macromolecules* **1996**, *29*, 3332−3333.

Table 3. Effect of Temperature and Ligand on Stereochemistry: [(BDI)ZnO^{i}Pr]$_2$ with Various Lactides[a]

entry	catalyst	monomer	temp (°C)	time (h)	conversion[b] (%)	M_n (kg/mol) (GPC)[c]	M_w/M_n (GPC)[c]	P_r[d]
1	[(BDI-**1**)ZnO^{i}Pr]$_2$	*rac*-LA	20	0.33	97	37.9	1.10	0.90
2	[(BDI-**2**)ZnO^{i}Pr]$_2$	*rac*-LA	20	8	97	42.5	1.09	0.79
3	[(BDI-**3**)ZnO^{i}Pr]$_2$	*rac*-LA	20	19	97	35.8	1.18	0.76
4	[(BDI-**1**)ZnO^{i}Pr]$_2$	*rac*-LA	0	2	97	38.8	1.09	0.94
5	[(BDI-**1**)ZnO^{i}Pr]$_2$	*meso*-LA	0	4	82	22.4	1.07	0.76
6[e]	[(BDI-**2**)ZnO^{i}Pr]$_2$	*meso*-LA	0	4	97	13.8	1.02	0.37

[a] [LA]/[Zn] = 200; T_{rxn} = 20 °C; [LA] = 0.4 M in CH_2Cl_2. [b] As determined via integration of the methyl resonances of LA and poly-LA ($CDCl_3$, 300 MHz). [c] Determined by gel-permeation chromatography, calibrated with polystyrene standards in tetrahydrofuran. [d] P_r is the probability of racemic linkages between monomer units and is determined from the methine region of the homonuclear decoupled ^{1}H NMR spectrum. [e] [LA]/[Zn] = 99.

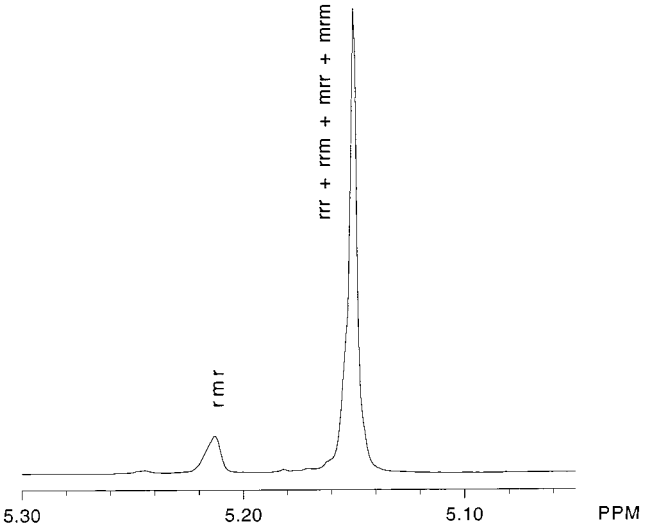

Figure 4. Homonuclear decoupled ^{1}H NMR spectrum of the methine region of syndiotactic PLA prepared from *meso*-LA with [(BDI-**1**)-ZnO^{i}Pr]$_2$ at 0 °C (500 MHz, $CDCl_3$).

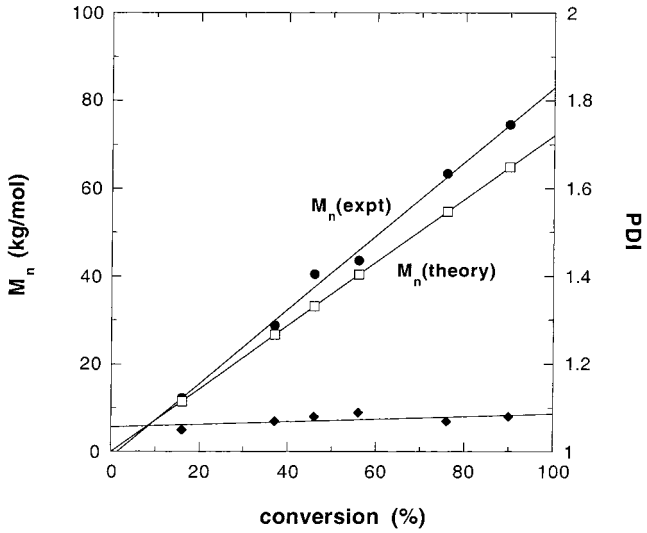

Figure 5. Plot of PLA M_n (versus polystyrene standards) and molecular weight distribution as a function of conversion with *rac*-LA and [(BDI-**1**)ZnO^{i}Pr]$_2$ (CH_2Cl_2, 20 °C, [LA]/[Zn] = 500).

analysis of oligomers formed by [(BDI-**1**)ZnO^{i}Pr]$_2$ ([LA]/[Zn] = 9) after quenching immediately with methanol) by electrospray-ionization mass spectrometry exhibited oligomers of the formula H(OCHMeCO)$_{2n}$O^{i}Pr·NH$_4^+$ (n = 3 to 12) as well as molecular ions corresponding to the methanolyzed ligand ((BDI-**1**)H$_2^+$) (Figure 6). Small peaks in the spectrum with masses intermediate to those of the primary species are due to transesterification during catalysis, while the other small envelope centered at *m*/*z* 840 and spaced by *m*/*z* 72 is due to unknown species that we believe form during quenching due to a zinc-catalyzed methanolysis of the oligomers. Analysis of oligomers formed by [(BDI-**1**)ZnO^{i}Pr]$_2$ at [LA]/[Zn] = 9 after reaction overnight revealed that transesterification is catalyzed by these complexes at longer reaction times, as oligomers of the formula H(OCHMeCO)$_n$O^{i}Pr·NH$_4^+$ were found.[32] This suggests that transesterification could degrade both the molecular weight distributions as well as stereochemistry of these polymers.[21] These data, along with fair agreement between observed and theoretical values of M_n, strongly support our hypothesis that [(BDI-**1**)ZnO^{i}Pr]$_2$ acts as a single-site catalyst wherein the bulky β-diiminate ligand remains bound to the zinc center while the isopropoxide ligand initiates polymerization.

Conversions of *rac*-lactide with time at various concentrations of [(BDI-**1**)ZnO^{i}Pr]$_2$ in methylene chloride at 25 °C were monitored by ^{1}H NMR spectroscopy until monomer consumption was complete ([LA]$_o$ = 1.026 M; [Zn] = 2.10 to 5.46 mM; [LA]/[Zn] = 488 to 188). In each case, first-order kinetics in monomer were observed; the appropriate semilogarithmic plots for several of these polymerizations are shown in Figure 7. Thus, the polymerization of *rac*-lactide by [(BDI-**1**)ZnO^{i}Pr]$_2$ presumably proceeds according to:

$$-\mathrm{d[LA]}/\mathrm{d}t = k_{app}[\mathrm{LA}]^1 \quad (1)$$

where $k_{app} = k_p[\mathrm{Zn}]^x$, and where k_p is the propagation rate constant. To determine the order in zinc (x), we plotted ln k_{app} versus ln [Zn] (Figure 8). From this plot, the order in initiator (slope) is 1.56 ± 0.06. Therefore, the polymerization of *rac*-lactide by [(BDI-**1**)ZnO^{i}Pr]$_2$ follows an overall kinetic law of the form:

$$-\mathrm{d[LA]}/\mathrm{d}t = k_p[\mathrm{Zn}]^{1.56}[\mathrm{LA}] \quad (2)$$

Fractional dependencies upon catalyst have been previously observed for ring-opening lactone polymerizations with related aluminum[18,42−45] and yttrium alkoxides;[9] in these systems, studies indicate that the observed kinetics result from aggregation of the active species in the polymerization medium.[44,45] We are currently investigating the nature of the active species in these polymerization systems, as they appear to be more complex than originally anticipated.

Conversion versus time data were also collected for the polymerization of *meso*- and (*S*,*S*)-lactide by [(BDI-**1**)ZnO^{i}Pr]$_2$ (CH_2Cl_2; 25 °C; [LA]$_o$ = 1.023, 1.005 M, respectively; [Zn] =

(42) Duda, A.; Penczek, S. *Macrmol. Rapid Commun.* **1994**, *15*, 559.
(43) Duda, A.; Penczek, S. *Polym. Prepr. (Am. Chem. Soc., Div. Polym. Chem.)* **1990**, *31*, 12.
(44) Ouhadi, T.; Hamitou, A.; Jerome, R.; Teyssie, P. *Macromolecules* **1976**, *9*, 927.
(45) Penczek, S.; Duda, A.; Biela, T. *Polym. Prepr. (Am. Chem. Soc., Div. Polym. Chem.)* **1994**, *35*, 508.

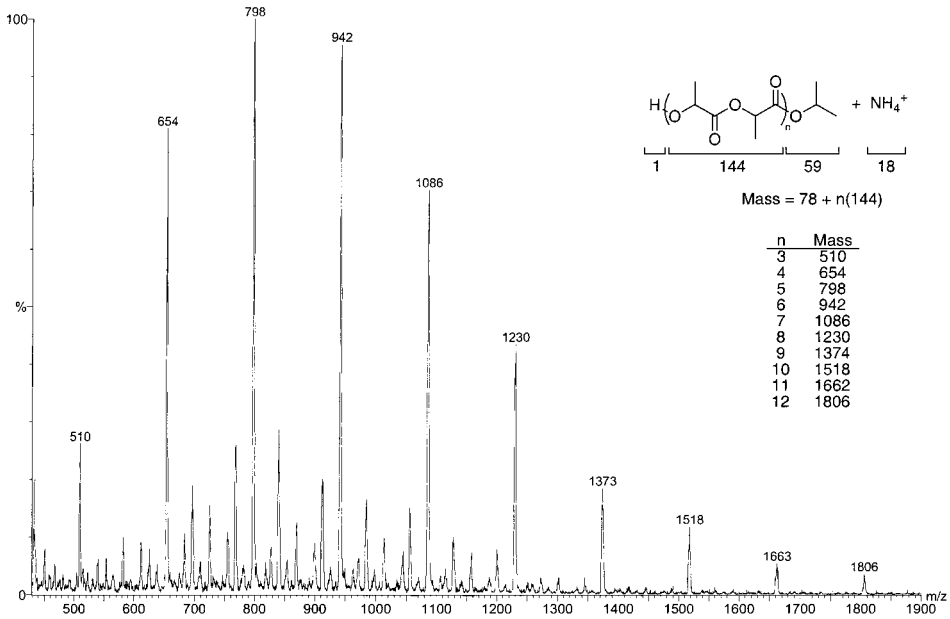

Figure 6. Electrospray MS of the crude reaction product of *rac*-lactide and [(BDI-**1**)ZnO^{i}Pr]$_2$ ([LA]/[Zn] = 9), quenched with methanol immediately after reaction is complete. Region *m*/*z* 430 to 1900.

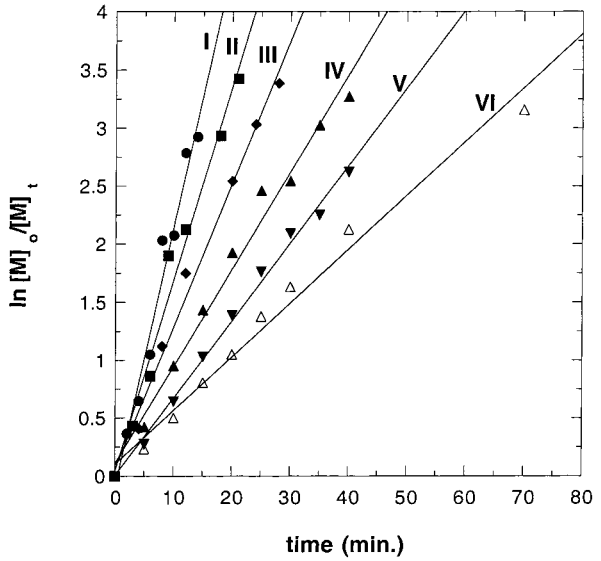

Figure 7. Semilogarithmic plots of *rac*-lactide conversion with time in CH_2Cl_2 at 25 °C with [(BDI-**1**)ZnO^{i}Pr]$_2$ as initiator ([LA]$_o$ = 1.026 M: **I**, [Zn] = 5.46 mM, [LA]/[Zn] = 188; **II**, [Zn] = 4.78 mM, [LA]/[Zn] = 215; **III**, [Zn] = 3.78 mM, [LA]/[Zn] = 271; **IV**, [Zn] = 3.18 mM, [LA]/[Zn] = 323; **V**, [Zn] = 2.57 mM, [LA]/[Zn] = 399; **VI**, [Zn] = 2.10 mM, [LA]/[Zn] = 488).

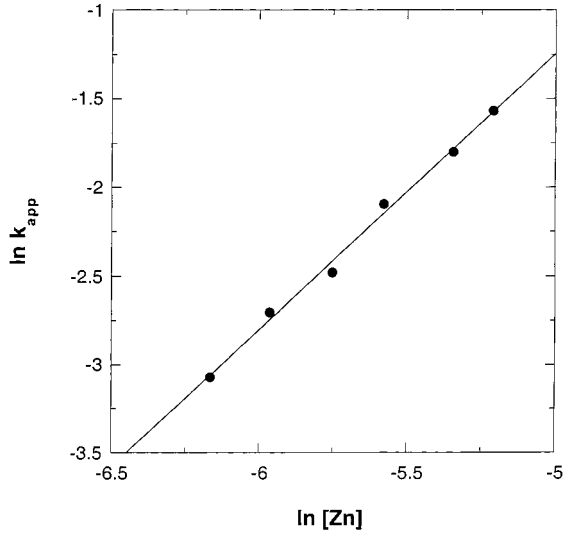

Figure 8. Plot of ln k_{app} versus ln [Zn] for the polymerization of *rac*-lactide with [(BDI-**1**)ZnO^{i}Pr]$_2$ as initiator (CH_2Cl_2, 25 °C, [LA]$_o$ = 1.026 M).

2.07, 5.39 mM, respectively; [LA]/[Zn] = 494, 186, respectively). In both cases, first-order kinetics in monomer were observed; the appropriate semilogarithmic plots for these polymerizations relative to *rac*-lactide are shown in Figures 9 and 10. Interestingly, the first-order rate constant (k_{app}) for the polymerization of *meso*-lactide (0.037 min^{-1}) is slightly smaller than that observed under identical conditions with *rac*-lactide (0.054 min^{-1}) ([LA]/[Zn] $\approx$ 490, [Zn] $\approx$ 2.1 mM; Figure 9). In contrast, the polymerization of (*S*,*S*)-lactide exhibits a k_{app} (0.031 min^{-1}) approximately seven times smaller than the observed k_{app} (0.22 min^{-1}) for the analogous polymerization with *rac*-lactide ([LA]/[Zn] $\approx$ 188, [Zn] $\approx$ 5.4 mM; Figure 10). These results agree well with our measured stereoselectivities. In particular, from the polymerization of *rac*-lactide, we observed that $k_{R/SS} \gg k_{R/RR}$ (or $k_{S/RR} \gg k_{S/SS}$). Thus, the polymerization of (*S*,*S*)-lactide should proceed significantly slower than that of *rac*-lactide. Specifically, the value of P_r = 0.90 for the polymerization of *rac*-lactide with [(BDI-**1**)ZnO^{i}Pr]$_2$ at 20 °C forecasts a relative rate difference of nine, which closely agrees with the observed value.

Finally, conversion versus time data were collected for the polymerization of *rac*-lactide with [(BDI-**2**)ZnO^{i}Pr]$_2$ and [(BDI-**3**)ZnO^{i}Pr]$_2$ (CH_2Cl_2; 25 °C; [LA]$_o$ = 1.023, 1.02 M, respectively; [Zn] = 5.44, 5.51 mM, respectively; [LA]/[Zn] = 188, 185, respectively). In both cases, first-order kinetics in monomer were observed; the appropriate semilogarithmic plots for these polymerizations are shown in Figure 11. From the kinetic data, it is apparent that the substituents on the β-diiminate ligand significantly affect the rate of polymerization. For instance, changing the ligand substituents from isopropyl to ethyl groups results in a decrease in k_{app} from 0.22 min^{-1} to 0.017 min^{-1}. Similarly, substitution with *n*-propyl groups lowers k_{app} to 0.0066 min^{-1}. These results reinforce recent reports that subtle ma-

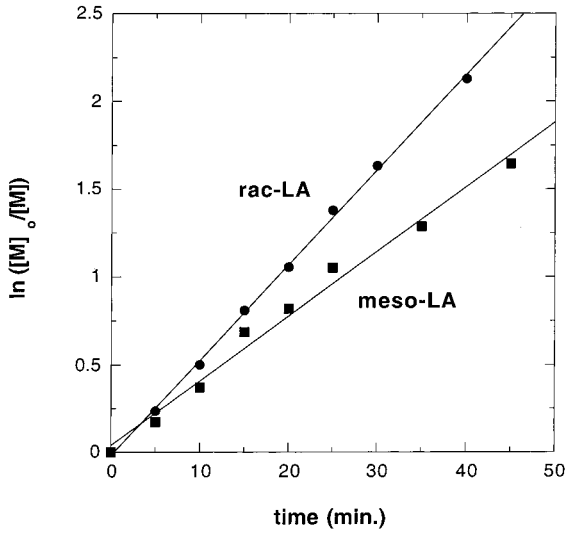

Figure 9. Semilogarithmic plots of *meso*- and *rac*-lactide conversion with time in CH_2Cl_2 at 25 °C with [(BDI-**1**)ZnO^{i}Pr]$_2$ as initiator ([LA]$_o$ = 1.023, 1.026 M, respectively; [Zn] = 2.07, 2.10 mM, respectively; [LA]/[Zn] = 494, 488, respectively).

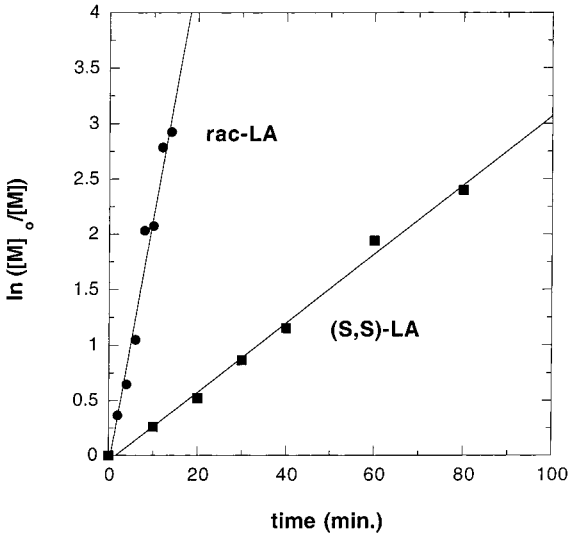

Figure 10. Semilogarithmic plots of (*S*,*S*)- and *rac*-lactide conversion with time in CH_2Cl_2 at 25 °C with [(BDI-**1**)ZnO^{i}Pr]$_2$ as initiator ([LA]$_o$ = 1.005, 1.026 M, respectively; [Zn] = 5.39, 5.46 mM, respectively; [LA]/[Zn] = 186, 188, respectively).

nipulations of ligand architecture can lead to drastic changes in lactide polymerization activity.[9,46]

Lactide Polymerization with [(BDI-1)MgO^{i}Pr]$_2$ Catalysts. Due to the successful implementation of tris(pyrazolyl)borato magnesium alkoxides as single-site catalysts for lactide polymerization,[7] we decided to investigate the synthesis of discrete β-diiminate magnesium alkoxides as catalysts for lactone polymerization.[47] On the basis of the synthesis of β-diiminate zinc alkoxides by the alcoholysis of complexes of the form (BDI)ZnR (R = alkyl, amido), we synthesized the analogous magnesium complexes. Reaction of (BDI-**1**)H with Mg[N(SiMe$_3$)$_2$]$_2$ yields (BDI-**1**)MgN(SiMe$_3$)$_2$ in an isolated yield of 84% following crystallization. We have not analyzed this compound by X-ray diffraction, but presume that it is a monomer analogous to (BDI-**1**)ZnN(SiMe$_3$)$_2$. Reaction with 2-propanol produces (BDI-**1**)MgO^{i}Pr in 65% isolated yield. The molecular structure of the complex was determined by X-ray diffraction to be an alkoxide-bridged dimer, virtually isostructural to [(BDI-**1**)Zn(O^{i}Pr)]$_2$[3] (Figure 12). The Mg−Mg separation is 3.01 Å, while Mg−O bonds are 1.98 and 1.99 Å, well within the acceptable range.[47] The six-membered chelate is puckered with a deviation of 0.78 Å from the plane of N(1)−N(2)−C(6). [(BDI-**1**)MgO^{i}Pr]$_2$ is highly active for the polymerization of *rac*-lactide; in 2 min at 20 °C, it polymerized *rac*-lactide to complete conversion to yield atactic PLA ([Mg] = 2 mM; [LA] = 0.4 M; [LA]/[Mg] = 200). Nonetheless, gel-

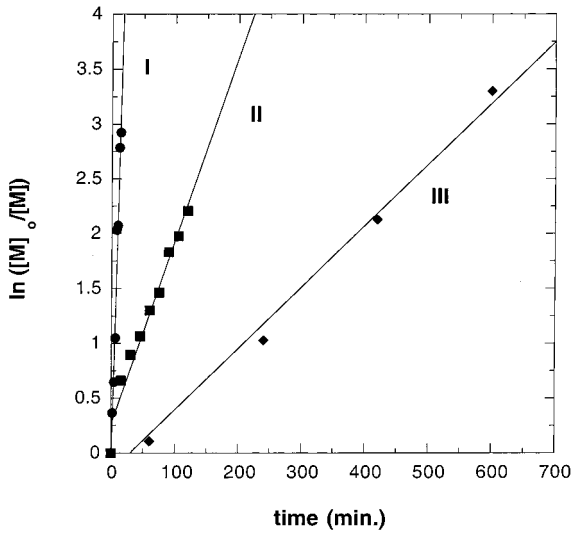

Figure 11. Semilogarithmic plots of *rac*-lactide conversion with time in CH_2Cl_2 at 25 °C (**I**: [(BDI-**1**)ZnO^{i}Pr]$_2$, [LA]$_o$ = 1.026 M, [Zn] = 5.46 mM, [LA]/[Zn] = 188; **II**: [(BDI-**2**)ZnO^{i}Pr]$_2$, [LA]$_o$ = 1.023 M, [Zn] = 5.44 mM, [LA]/[Zn] = 188; **III**: [(BDI-**3**)ZnO^{i}Pr]$_2$, [LA]$_o$ = 1.02 M, [Zn] = 5.51 mM, [LA]/[Zn] = 185).

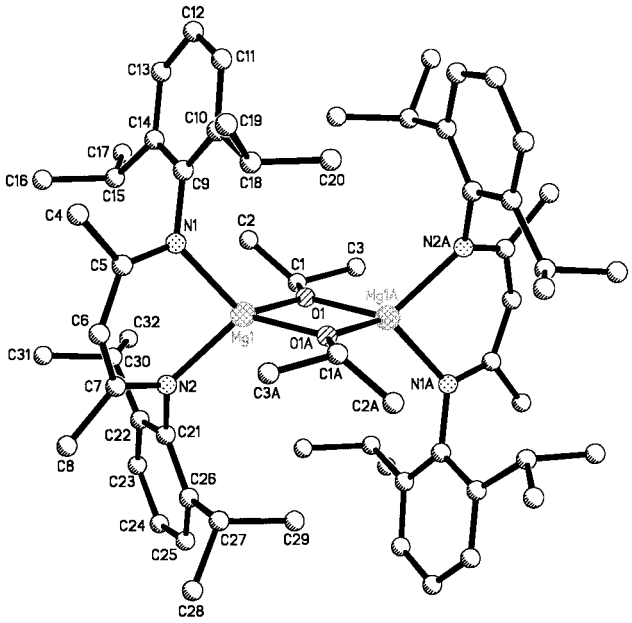

Figure 12. X-ray crystal structure of [(BDI-**1**)Mg(O^{i}Pr)]$_2$. Selected bond lengths (Å) and bond angles (deg): Mg(1)−N(1) 2.123(3), Mg(1)−N(2) 2.114(3), Mg(1)−O(1) 1.978(2), Mg(1)−O(1A) 1.987(2), N(1)−Mg(1)−N(2) 91.27(10), O(1)−Mg(1)−O(1A) 80.95(9), N(1)−Mg(1)−O(1) 126.19(10), N(2)−Mg(1)−O(1) 123.44(10), Mg(1)−O(1)−Mg(1A) 99.05(9).

(46) Bhaw-Luximon, A.; Jhurry, D.; Spassky, N. *Polym. Bull.* **2000**, *44*, 31−38.

(47) For recent reports of magnesium complexes with β-diiminate ligands, see: (a) Bailey, P. J.; Dick, C. M. E.; Fabre, S.; Parsons, S. *J. Chem. Soc.; Dalton Trans.* **2000**, *10*, 1655−1661. (b) Gibson, V. C.; Segal, J. A.; White, A. J. P.; Williams, D. J. *J. Am. Chem. Soc.* **2000**, *122*, 7120−7121.

Table 4. Polymerization of *rac*-Lactide using [(BDI-**1**)MgO^{i}Pr]$_2$/2-Propanol[a]

entry	[LA]:[Mg]:[^{i}PrOH]	time (min)	conversion[b] (%)	M_n (kg/mol) (GPC)[c]	M_w/M_n (GPC)[c]
1	50:1:1	1	97	11.0	1.20
2	100:1:1	2	97	17.7	1.28
3	200:1:1	2	97	29.7	1.29
4	300:1:1	5	98	39.8	1.33
5	500:1:1	5	96	55.3	1.35

[a] T_{rxn} = 20 °C; [LA] = 0.4 M in CH_2Cl_2. [b] As determined via integration of the methyl resonances of LA and poly-LA ($CDCl_3$, 300 MHz). [c] Determined by gel-permeation chromatography, calibrated with polystyrene standards in tetrahydrofuran.

permeation chromatography (GPC, versus polystyrene standards) revealed an M_n of 64 000 g/mol (M_n theory = 28 800 g/mol) and a molecular weight distribution of 1.59. We tentatively attribute the broad molecular weight distribution of this polymer to slow initiation (relative to propagation) of the complex as well as transesterification reactions. However, polymerization of *rac*-lactide with [(BDI-**1**)MgO^{i}Pr]$_2$ and 1 equiv of 2-propanol led to the formation of narrow molecular weight distribution PLA with molecular weights that agree well with theoretical values (Table 4). These results show that 2-propanol can interact with and modify the reactivity of [(BDI-**1**)MgO^{i}Pr]$_2$. Regardless of the mechanism of polymerization, these complexes exhibit polymerization rates that are among the highest reported.[48] It is currently unclear why the structurally similar zinc complex exhibits heterospecific chain-end control in the polymerization of *rac*-lactide while the magnesium complex does not exhibit chain-end control under the conditions employed.

Summary and Perspective

In conclusion, we report a series of zinc alkoxide complexes that act as single-site, living initiators for the polymerization of (*S*,*S*)-lactide to isotactic PLA, *rac*-lactide to heterotactic PLA, and *meso*-lactide to syndiotactic PLA. Microstructural analysis of the polymers formed by these complexes reveals that the β-diiminate ligands exert significant influence on the tacticity of the growing polymer chains. Furthermore, kinetic analysis suggests that, although polymerizations of *rac*-lactide by these complexes are first order in monomer, the active initiating species are much more complex than previously anticipated in the polymerization medium. Finally, microstructural and kinetic data indicate that the substituents on the β-diiminate ligand significantly affect catalytic activity as well as the ability of the zinc-based complexes to control the stereochemistry of monomer enchainment, while interestingly we do not observe stereochemical control with the magnesium analogues. Future work will be directed toward understanding the significant differences between these structurally similar zinc and magnesium complexes, as well as to discover new metal-based lactide polymerization catalysts employing the β-diiminate ligand structure. Our studies not only represent important progress in understanding the core issues surrounding the selectivity and mechanism of lactide polymerization but also provide a firm foundation for the further development of single-site catalysts for the construction of PLA and other new polyester architectures.

Experimental Section

General Considerations. All reactions with air- and/or water-sensitive compounds were carried out under dry nitrogen with drybox or standard Schlenk line techniques. NMR spectra were recorded on a Bruker AF300 (^{1}H, 300 MHz; ^{13}C, 75 MHz) or a Varian INOVA400 (^{1}H, 400 MHz; ^{13}C, 100 MHz) spectrometer, and are referenced versus shifts of solvents containing residual protic impurities. Gel permeation chromatography (GPC) analyses were carried out on a Waters instrument (M510 pump, U6K injector) equipped with Waters UV486 and Milton Roy differential refractive index detectors, and four 5 μm PL Gel columns (Polymer Laboratories; 100 Å, 500 Å, 1000 Å, and Mixed C porosities) in series. The GPC columns were eluted with tetrahydrofuran at 45 °C at 1 mL/min and were calibrated with 23 monodisperse polystyrene standards. Crystallographic data were collected with a SMART CCD Area Detector System (Mo Kα, λ = 0.71073 Å), and frames were integrated with the Siemens SAINT program. Electrospray-ionization mass spectrometry was carried out on a Micromass Quattro I mass spectrometer operated in positive-ion mode. Samples were dissolved in acetonitrile with a trace of ammonium hydroxide and were infused with a syringe pump at 5μL/min (source temperature 80 °C; cone voltage 19 V).

Materials. Hexanes and methylene chloride were distilled from CaH_2 under nitrogen, while toluene was distilled from sodium ketyl under nitrogen. *rac*- and (*S*,*S*)-lactide were purchased from Purac USA and sublimed prior to use. *meso*-lactide was prepared by published procedures.[4] 2-((2,6-Diisopropylphenyl)amino)-4-((2,6-diisopropylphenyl)imino)-2-pentene (BDI-**1**)H and (BDI-**2**)H were prepared by procedures analogous to those described in the literature.[49] 2,6-Diallylaniline was prepared according to the published procedure.[50] Zinc bis(trimethylsilyl)amide and *rac*-methyl lactate were purchased from Aldrich and used as received. Magnesium bis(trimethylsilyl)amide was prepared as described in the literature.[51] Anhydrous 2-propanol was purchased from Acros and used as received. (BDI-**1**)ZnN(SiMe$_3$)$_2$,[3] [(BDI-**1**)ZnO^{i}Pr]$_2$,[3] and [(BDI-**1**)ZnOAc]$_2$[34] were prepared according to published procedures.

2,6-Di-*n*-propylaniline. 2,6-Diallylaniline (3.76 g, 21.7 mmol) was dissolved in absolute ethanol and transferred to a Fischer−Porter bottle equipped with a pressure fitting rated to 100 psi. After addition of 10% palladium on carbon (0.100 g), the reactor was pressured to 100 psi with H_2. The reaction was then stirred at room temperature, with periodic refilling of H_2, until the pressure remained constant. Following the release of pressure, the solvent was removed in vacuo to afford a dark orange oil. This oil was dissolved in diethyl ether (20 mL) and treated with gaseous HCl, resulting in a flocculent white precipitate. This precipitate was collected by filtration, suspended in diethyl ether (20 mL), and then washed with saturated aqueous bicarbonate (3 × 10 mL) followed by brine (1 × 25 mL). The organic layer was separated, dried over Na_2SO_4, and filtered. Following removal of the solvent in vacuo, the resulting oil was distilled (bp 110 °C/60 mmHg) to afford the title compound as a light brown oil (3.08 g, 80% yield). ^{1}H NMR (C_6D_6, 300 MHz): δ 6.93 (2H, d, J = 7.5 Hz, ArH), 6.77 (1H, t, J = 7.5 Hz, ArH), 3.10 (2H, br, NH_2), 2.27 (4H, t, J = 7.5 Hz, CH_2CH$_2$CH$_3$), 1.52 (4H, sextet, J = 7.5 Hz, CH$_2$CH_2CH$_3$), 0.86 (6H, t, J = 7.3 Hz, CH$_2$CH$_2$CH_3) ppm.

2-((2,6-Di-*n*-propylphenyl)amino)-4-((2,6-di-*n*-propylphenyl)-imino)-2-pentene (BDI-3)H. 2,6-Di-*n*-propylaniline (2.36 g, 13.3 mmol), 2,4-pentanedione (0.668 g, 6.67 mmol), and concentrated HCl (0.59 mL) were combined in absolute ethanol (10 mL) and heated at reflux for 3 days. After being cooled to room temperature, the orange solution was concentrated and hexanes (50 mL) were added. The resulting precipitate was collected by filtration, suspended in diethyl ether (20 mL), and washed with saturated aqueous bicarbonate (3 × 10 mL) followed by brine (1 × 25 mL). The organic layer was separated, dried over Na_2SO_4, and filtered. Removal of the solvent in vacuo afforded (BDI-**3**)H as a light brown oil (1.50 g, 54% yield). ^{1}H NMR (C_6D_6, 300 MHz): δ 12.20 (1H, s, NH), 7.08 (6H, br, ArH), 4.83 (1H, s, β-CH), 2.60 (8H, m, CH_2CH$_2$CH$_3$), 1.64 (14H, br, α-Me, CH$_2$CH_2CH$_3$), 0.97 (12H, t, J = 7.5 Hz, CH$_2$CH$_2$CH_3) ppm.

(48) McLain, S. L.; Ford, T. M.; Drysdale, N. E. *Polym. Prepr. (Am. Chem. Soc., Div. Polym. Chem.)* **1992**, *33* (2), 463−464.

(49) Feldman, J.; McLain, S. J.; Parthasaranthy, A.; Marshall, W. J.; Calabrese, J. C.; Arthur, S. D. *Organometallics* **1997**, *16*, 1514−1516.

(50) Arestat, G. *Synth. React. Inorg. Met. Org. Chem.* **1979**, *9*, 377−390.

(51) Allan, J. F.; Henderson, K. W.; Kennedy, A. R. *Chem. Commun.* **1999**, 1325−1326.

(BDI-2)ZnN(SiMe$_3$)$_2$. To a solution of (BDI-**2**)H (3.54 g, 9.77 mmol) in toluene (15 mL) was added zinc bis(trimethylsilyl)amide (3.95 mL, 9.79 mmol) in toluene (5 mL). After being stirred for 18 h at 70 °C, the clear yellow solution was dried in vacuo, giving (BDI-**2**)ZnN(SiMe$_3$)$_2$ in quantitative yield (5.74 g). The light yellow solid was recrystallized from hexanes at −5 °C to yield colorless blocks (3.59 g, 62% yield). ^{1}H NMR (C_6D_6, 300 MHz): δ 7.11 (6H, br, ArH), 4.87 (1H, s, β-C*H*), 2.73 (4H, m, J = 7.5 Hz, CH_2CH$_3$), 2.60 (4H, m, J = 7.5 Hz, CH_2CH$_3$), 1.58 (6H, s, α-Me), 1.21 (12H, t, J = 7.5 Hz, CH$_2$CH_3), 0.03 (18H, s, CH_3) ppm. ^{13}C{^{1}H} NMR (C_6D_6, 75 MHz): δ 169.21, 145.86, 136.99, 125.99, 125.85, 95.62, 24.79, 23.43, 13.59, 5.17 ppm.

(BDI-3)ZnN(SiMe$_3$)$_2$. To a solution of (BDI-**3**)H (0.523 g, 1.25 mmol) in toluene (5 mL) was added zinc bis(trimethylsilyl)amide (0.505 mL, 1.25 mmol) in toluene (5 mL). After being stirred for 18 h at 80 °C, the clear yellow solution was dried in vacuo, giving (BDI-**3**)ZnN(SiMe$_3$)$_2$ in quantitative yield (0.804 g). ^{1}H NMR (C_6D_6, 300 MHz): δ 7.11 (6H, br, ArH), 4.90 (1H, s, β-C*H*), 2.69 (4H, t, J = 7.5 Hz, CH_2CH$_2$CH$_3$), 1.64 (14H, s, α-Me, CH$_2$CH_2CH$_3$), 0.99 (12H, t, J = 7.5 Hz, CH$_2$CH$_2$CH_3), 0.02 (18H, s, CH_3) ppm.

[(BDI-2)ZnO^{i}Pr]$_2$. To a solution of (BDI-**2**)ZnN(SiMe$_3$)$_2$ (0.449 g, 0.764 mmol) in toluene (6 mL) was added 2-propanol (58 μL, 0.763 mmol). After the solution was stirred at room temperature for 1 h, the resulting slurry was dried in vacuo. The white solid was recrystallized from toluene (10 mL) at −5 °C to yield [(BDI-**2**)ZnO^{i}Pr]$_2$ as colorless blocks (0.25 g, 67% yield). ^{1}H NMR (CD_2Cl_2, 300 MHz) δ 7.11 (6H, br, ArH), 4.74 (1H, s, β-C*H*), 3.46 (1H, m, J = 5.9 Hz, OC*H*Me$_2$), 2.45 (4H, m, J = 7.5 Hz, CH_2CH$_3$), 1.94 (4H, m, J = 7.5 Hz, CH_2-CH$_3$), 1.41 (6H, s, α-Me), 0.98 (12H, t, J = 7.5 Hz, CH$_2$CH_3), 0.81 (6H, d, J = 5.9 Hz, OCH*Me*$_2$) ppm. ^{13}C{^{1}H} NMR (C_6D_6, 75 MHz): δ 167.51, 147.72, 137.61, 125.52, 124.42, 94.78, 65.04, 27.79, 23.53, 23.49, 13.60 ppm. X-ray analysis of the crystals revealed that the complex exists as a μ-isopropoxide-bridged dimer in the solid state (see Supporting Information).

[(BDI-3)ZnO^{i}Pr]$_2$. To a solution of (BDI-**3**)ZnN(SiMe$_3$)$_2$ (0.80 g, 1.24 mmol) in toluene (6 mL) was added 2-propanol (95 μL, 1.24 mmol). After the mixture was stirred at room temperature for 1 h, the resulting slurry was dried in vacuo. The white solid was recrystallized from hexanes (10 mL) at 20 °C to yield [(BDI-**3**)ZnO^{i}Pr]$_2$ as colorless blocks (0.360 g, 54% yield). ^{1}H NMR (C_6D_6, 300 MHz): δ 7.17 (6H, br, ArH), 4.72 (1H, s, β-C*H*), 3.83 (1H, septet, J = 5.9 Hz, OC*H*Me$_2$), 2.71 (4H, m, CH_2CH$_2$CH$_3$), 2.04 (4H, m, CH_2CH$_2$CH$_3$), 1.67 (8H, m, CH$_2$CH_2CH$_3$), 1.46 (6H, s, α-Me), 1.18 (6H, d, J = 5.9 Hz, OCH*Me*$_2$), 0.99 (12H, t, J = 7.2 Hz, CH$_2$CH$_2$CH_3) ppm. ^{13}C{^{1}H} NMR (C_6D_6, 75 MHz): δ 167.90, 148.17, 136.85, 128.45, 128.32, 128.00, 127.87, 127.81, 127.69, 126.61, 124.33, 118.93, 118.86, 94.68, 65.22, 32.88, 24.06, 23.10, 14.69 ppm. X-ray analysis of the crystals revealed that the complex exists as a μ-isopropoxide-bridged dimer in the solid state (see Supporting Information).

***rac*-(BDI-1)ZnOCH(Me)CO$_2$Me.** To a solution of (BDI-**1**)ZnN(SiMe$_3$)$_2$ (0.452 g, 0.703 mmol) in toluene (6 mL) was added *rac*-methyl lactate (74 μL, 0.704 mmol). After the mixture was stirred for 5 h at room temperature, the resulting slurry was dried in vacuo. Hexanes (20 mL) were added, and the precipitate was filtered through a pad of Celite. The filtrate was then concentrated and cooled to −5 °C, whereupon *rac*-(BDI-**1**)ZnOCH(Me)CO$_2$Me crystallized as colorless blocks (0.167 g, 41% yield). ^{1}H NMR (C_6D_6, 300 MHz): δ 7.08 (6H, m, ArH), 4.94 (1H, s, β-C*H*), 4.29 (1H, quartet, J = 7.0 Hz; OC*H*MeCO$_2$Me), 3.41 (4H, m, J = 7.0 Hz, C*H*Me$_2$), 3.14 (3H, s, CO$_2$-Me), 1.73 (6H, s, α-Me), 1.41 (6H, d, J = 7.0 Hz, CH*Me*Me), 1.32 (6H, d, J = 7.0 Hz, CH*Me*Me), 1.19 (6H, d, J = 7.0 Hz, CHMe*Me*), 1.16 (6H, d, J = 7.0 Hz, CHMe*Me*), 0.70 (3H, d, J = 7.0 Hz, OCH*Me*CO$_2$Me) ppm. ^{13}C{^{1}H} NMR (C_6D_6, 75 MHz): δ 168.79, 144.43, 142.75, 142.56, 125.83, 123.89, 123.78, 93.98, 70.64, 52.88, 28.22, 28.17, 24.66, 24.48, 24.43, 23.72, 23.56 ppm (one resonance missing possibly due to low resolution). X-ray analysis of the crystals revealed that the complex exists as a monomer in the solid state (see Supporting Information).

(BDI-1)ZnEt. To a solution of diethyl zinc (0.61 mL, 5.95 mmol) in toluene (10 mL) was slowly added (BDI-**1**) (0.501 g, 1.196 mmol) in toluene (10 mL) at 0 °C. After the mixture was stirred for 18 h at 80 °C, the clear solution was dried in vacuo giving (BDI-**1**)ZnEt as a viscous yellow oil in quantitative yield (0.612 g). This oil crystallized as large blocks upon standing over the course of several weeks. ^{1}H NMR (C_6D_6, 300 MHz): δ 7.07 (6H, m, ArH), 4.98 (1H, s, β-C*H*), 3.18 (4H, m, C*H*Me$_2$), 1.69 (6H, s, α-Me), 1.25 (12H, d, J = 7.0 Hz, CH*Me*Me), 1.14 (12H, d, J = 7.0 Hz, CHMe*Me*), 0.89 (3H, t, J = 8.0 Hz, CH$_2$CH_3) ppm. ^{13}C{^{1}H} NMR (C_6D_6, 75 MHz): δ 167.03, 144.67, 141.17, 125.61, 123.46, 95.03, 28.16, 23.88, 23.14, 22.93, 11.74, −1.53 ppm.

(BDI-1)MgN(SiMe$_3$)$_2$. To a solution of (BDI-**1**)H (2.045 g, 4.883 mmol) in toluene (20 mL) was added a solution of magnesium bis(trimethylsilyl)amide (1.707 g, 4.947 mmol) in toluene (20 mL). After the mixture was stirred for 18 h at 80 °C, the solvent was removed in vacuo to give (BDI-**1**)MgN(SiMe$_3$)$_2$ in quantitative yield. The light yellow solid was recrystallized from toluene at −30 °C to yield colorless blocks (2.48 g, 84% yield). ^{1}H NMR (C_6D_6, 300 MHz): δ 7.12 (6H, br, ArH), 4.80 (1H, s, β-C*H*), 3.20 (4H, m, J = 7.0 Hz, C*H*Me$_2$), 1.62 (6H, s, α-Me), 1.36 (12H, d, J = 7.0 Hz, CH*Me*Me), 1.14 (12H, d, J = 7.0 Hz, CHMe*Me*), 0.01 (18H, s, CH$_3$) ppm. ^{13}C{^{1}H} NMR (C_6D_6, 75 MHz): δ 170.43, 144.19, 141.86, 125.72, 123.95, 95.29, 28.69, 24.57, 24.39, 24.29, 5.05 ppm.

[(BDI-1)MgO^{i}Pr]$_2$. To a solution of (BDI-**1**)MgN(SiMe$_2$)$_2$ (0.558 g, 0.926 mmol) in toluene (8 mL) was added 2-propanol (78 μL, 1.03 mmol). After the mixture was stirred for 4 h at room temperature, the resulting white slurry was dried in vacuo. The white solid was then recrystallized from toluene (30 mL) at room temperature to yield [(BDI-**1**)MgO^{i}Pr]$_2$ as colorless blocks (0.302 g, 65% yield). ^{1}H NMR (toluene-d_8, 300 MHz): δ 7.07 (6H, m, ArH), 4.78 (1H, s, β-C*H*), 3.87 (1H, m, J = 6.0 Hz, OC*H*Me$_2$), 3.45 (2H, m, J = 7.0 Hz, C*H*Me$_2$), 3.11 (2H, m, J = 7.0 Hz, C*H*Me$_2$), 1.45 (6H, s, α-Me), 1.36 (6H, d, J = 7.0 Hz, CH*Me*Me), 1.23 (6H, d, J = 6.0 Hz, OCH*Me*$_2$), 1.16 (6H, d, J = 7.0 Hz, CH*Me*Me), 1.07 (6H, d, J = 7.0 Hz, CHMe*Me*), 0.40 (6H, d, J = 7.0 Hz, CHMe*Me*) ppm. ^{13}C{^{1}H} NMR (toluene-d_8, 75 MHz): δ 169.25, 161.15, 146.49, 142.42, 140.89, 137.51, 136.05, 128.95, 128.19, 125.49, 125.32, 123.65, 123.23, 123.02, 93.90, 53.60, 28.28, 28.00, 24.13, 23.40, 23.09, 22.77, 21.05, 20.42, 20.14 ppm. X-ray analysis of the crystals revealed that the complex exists as a μ-isopropoxide-bridged dimer in the solid state (see Supporting Information).

General Polymerization Procedure. A Schlenk flask was charged with a 34 mM solution of the catalyst in methylene chloride. To this solution was added a 0.40 M solution of monomer in methylene chloride ([monomer]:[Zn] = 200:1). The reaction was stirred at the desired temperature for the desired reaction time. After a small sample of the crude material was removed for characterization, the reaction was quenched with methanol (1 mL), the solution was concentrated in vacuo, and the polymer was precipitated with excess methanol. The polymer was then dried in vacuo to constant weight.

General Kinetic Procedure. A solution of catalyst in methylene chloride (5 mL) was added to monomer (13 mL of a 1.39 M solution in methylene chloride; resultant [LA]$_o$ = 1.0 M). The mixture was then stirred at 25 °C under N$_2$. At appropriate time intervals, 0.5 mL aliquots were removed and quenched with methanol (3 drops). The aliquots were then dried to constant weight in vacuo and analyzed by ^{1}H NMR.

X-ray Crystallography. Suitable crystals of each sample were attached to a glass fiber with heavy-weight oil and mounted in the Siemens SMART system for data collection at 173(2) K. Initial sets of cell constants for each sample were calculated from reflections harvested from three sets of 20 frames. These initial sets of frames were oriented such that orthogonal wedges of reciprocal space were surveyed. This produced orientation matrices from 248 reflections. In each case, final cell constants were calculated from a set of no less than 5000 strong reflections from the actual data collections. For each sample, a randomly oriented region of reciprocal space was surveyed to the extent of 1.3 hemispheres to a resolution of 0.84 Å. Three major swaths of frames were collected with 0.30° steps in ω.

Space groups for each sample were determined on the basis of systematic absences and intensity statistics. In each case, successful direct-methods solutions were calculated which provided most non-hydrogen atoms from the E-map. Several full-matrix least-squares/difference Fourier cycles were then performed to locate the remainder of the non-hydrogen atoms. For each sample, all non-hydrogen atoms

were refined with anisotropic displacement parameters, and all hydrogen atoms were placed in ideal positions and refined as riding atoms with individual (or group if appropriate) isotropic displacement parameters.

Complete drawings and full details of the X-ray structure determinations, including tables of bond lengths and angles, atomic positional parameters, and final thermal parameters for [(BDI-**2**)ZnO^{i}Pr]$_2$, [(BDI-**3**)ZnO^{i}Pr]$_2$ *rac*-(BDI-**1**)ZnOCHMeCO$_2$Me and [(BDI-**1**)MgO^{i}Pr]$_2$ are provided in the Supporting Information.

Acknowledgment. This work was generously supported by the NSF (Career Award CHE-9875261). We thank the Cornell University Center for Biotechnology, a New York State Center for Advanced Technology supported by the New York State Science and Technology Foundation, and industrial partners for partial support of this research. This work made use of the Cornell Center for Materials Research Shared Experimental Facilities, supported through the National Science Foundation Materials Research Science and Engineering Centers program (DMR-0079992), and the Cornell Chemistry Department X-ray Facility (supported by the NSF; CHE-9700441). G.W.C. gratefully acknowledges a Camille and Henry Dreyfus New Faculty Award, a Research Corporation Research Innovation Award, an Alfred P. Sloan Research Fellowship, an Arnold and Mabel Beckman Foundation Young Investigator Award, a Camille Dreyfus Teacher-Scholar Award, a 3M Untenured Faculty Grant, an IBM Partnership Award, and a Union Carbide Innovation Recognition Award. We thank Dr. Athula Attygalle for assistance with obtaining mass spectroscopy data, and Joseph Reczek for assistance with ligand synthesis.

Supporting Information Available: Polymer analysis data (MS/NMR spectra) and crystal structure data for [(BDI-**2**)ZnO^{i}Pr]$_2$, [(BDI-**3**)ZnO^{i}Pr]$_2$, *rac*-(BDI-**1**)ZnOCHMeCO$_2$Me, and [(BDI-**1**)MgO^{i}Pr]$_2$ (PDF). This material is available free of charge via the Internet at http://pubs.acs.org.

JA003851F